The application of the synergistic effect between the crystal structure of poly(lactic acid) (PLA) and the presence of ethylene vinyl acetate copolymer (EVA) to produce highly ductile PLA/EVA blends

Tamás Tábi[1,2]

Abstract

In this paper, we produced ethylene vinyl acetate copolymer (EVA)-filled poly(lactic acid) (PLA) blends by extrusion and injection moulding. We annealed the injection-moulded specimens at 80 °C, 100 °C, 120 °C and 140 °C to produce various crystal structures in PLA. Then we investigated the cross-effect between the crystal structure of PLA and the presence of EVA on the mechanical, impact, calorimetric, thermomechanical and heat deflection temperature properties of the blends. We found a synergistic toughening effect between the crystal structure of PLA that developed during annealing and the presence of dispersed EVA particles in the PLA matrix. The blend had a very high impact strength of over 65 kJ m^{-2}, which is three times higher than the impact strength of acrylonitrile butadiene styrene copolymer (~ 20 kJ m^{-2}), and thus it is very promising for technical applications.

Keywords Biopolymer · Poly(lactic acid) · Ethylene vinyl acetate · Crystal structure · Annealing · Improved toughness

Introduction

Nowadays, renewable resource-based and inherently biodegradable polymers, or biopolymers, are attracting more and more interest, since they are believed to replace petroleum-based "ordinary" plastics in the future and solve or at least ease waste management problems caused by the accumulation of non-biodegradable, short-lifetime plastic products. Due to the fact that biopolymers can be both renewable resource based and biodegradable at the same time, they can fit into the concept of sustainability and environmental consciousness [1–5].

Currently, one of the most suitable biopolymers to replace petroleum-based plastics is poly(lactic acid) (PLA) [6]. Lactic acid can be produced by the fermentation of glucose (derived from agricultural products like sugar or starch) in the presence of lactobacillus, which can be further used to produce PLA through direct polycondenzation or first by producing lactide (dimer of lactic acid) and then by its ring-opening polymerization. Usually, the latter method is applied to synthetize high molecular weight PLA. Since lactic acid has two stereoisomers named L-lactic acid and D-lactic acid and three dimers accordingly (L-lactide, D-lactide and meso-lactide), thus a variety of PLA polymers can be synthetized. Moreover, PLA itself can be considered a copolymer of L- and D-lactic acid (or L-, and D-lactide). Usually, a commercially available PLA grade contains around 1–15% D-lactide depending on the application needed, since D-lactide content influences crystallization behaviour among other thermal and mechanical properties. Below 1% D-lactide content, the given PLA grade is practically isotactic and is thus called poly(L-lactic acid) (PLLA) [7].

PLA is a thermoplastic, aliphatic, semi-crystalline polyester with a generally slow crystallization rate dependent on D-lactide content [8–10]. According to its crystal structure, PLA can crystallize into various crystal forms named α, β, γ and η (or called stereocomplex) [11]. The most common and stable polymorph is the α form (orthorhombic unit cell), which develops when PLA is

✉ Tamás Tábi
tabi@pt.bme.hu

1   MTA–BME Research Group for Composite Science and Technology, Műegyetem rkp. 3., Budapest 1111, Hungary

2   Department of Polymer Engineering, Faculty of Mechanical Engineering, Budapest University of Technology and Economics, Műegyetem rkp. 3., Budapest 1111, Hungary

crystallized from melt, from solution or cold-crystallized in solid state [12, 13]. Additionally, it was also reported [14–16] that PLA could also crystallize into a less ordered or disordered crystal named α′, which has the same conformation, but a loose packing manner and lower density compared to the more ordered α crystal form. On the contrary, the β form (trigonal unit cell) develops when high drawing and high temperature are applied to the α form [17, 18], while the γ form (orthorhombic unit cell) can be developed by epitaxial crystallization on a hexa-methyl-benzene substrate [19]. Finally, the η form or stereocomplex crystal structure develops when the optically pure PLLA and PDLA (poly(D-lactic acid)) are melt-blended [20–22]. Besides this special stereocomplex crystalline structure, most research concentrated on the α crystal form since this type develops during the melt processing of PLA, like injection moulding, during cold crystallization (annealing), and also in most cases when nucleating agents are used [23], and thus this one has the most practical significance related to processing.

PLA has high strength ($\sim$ 60 to 65 MPa) and high modulus ($\sim$ 2.5 to 3.0 GPa), which makes it suitable for applications like bottles, office utensils, cups and trays. By modifications like plasticizing or flame retarding, it can even be used as a film for food packaging [24], or in electronic and automotive applications [25]. Nevertheless, PLA also has two main drawbacks that highly limit its widespread application: its low heat deflection temperature (HDT) ($\sim$ 50 to 55 °C) and low impact strength ($\sim$ 3 kJ m^{-2} notched Charpy impact strength) [6]. The low HDT of the PLA products is caused by two properties. Firstly, by the slow crystallization rate of PLA, which induces only very low crystallinity during melt processing like injection moulding and, secondly, by its inherently low glass transition temperature (T_g) of around 55 °C. One possibility to overcome low HDT is to crystallize (anneal or cold crystallize) the final PLA product after production in a heated chamber above its T_g to develop a highly crystalline structure. In our previous publication [26], it was pointed out that according to the annealing temperature applied, the HDT of the annealed part could be highly influenced in a broad range. It was also found that the HDT of PLA parts is not only influenced by crystallinity, but also by crystal structure (ratio of α′ and α crystal forms), where both are dependent on the annealing temperature applied. Moreover, annealing not only influences HDT, but also improves the impact strength of PLA, since during fracture, the crack propagates most probably in the boundary surface of the developed spherulites.

Although annealing was found to be an effective tool to overcome the low HDT of PLA products, at the same time, annealing is not enough to improve the impact strength of PLA to a desired level, such as the impact strength of the widely used tough polymer acrylonitrile butadiene styrene copolymer (ABS) ($\sim$ 20 kJ m^{-2} notched Charpy impact strength). One possible way to improve the impact properties of PLA is to add low-modulus and high-toughness polymers like ethylene vinyl acetate copolymer (EVA) [27–35]. EVA is a copolymer of ethylene and vinyl acetate, and it is a thermoplastic elastomer (not vulcanized) with high flexibility and toughness, widely used in the plastic industry. The mass percent of the vinyl acetate (VA) co-monomer can be varied in a broad range, while the other co-monomer is ethylene. With increasing VA content, the EVA copolymer changes from a semi-crystalline thermoplastic polymer (low-density polyethylene (LDPE)) into a rubber and again into an amorphous thermoplastic polymer (poly(vinyl acetate) (PVA)) [36]. Since PLA is miscible with PVA [37] and exhibits phase separation when blended with LDPE [38], the compatibility between PLA and EVA can be tuned with the VA content of EVA, without the need for a further compatibilizer.

In the research of Ma et al. [27], the VA content of PLA/EVA (80/20 mass%) blends was investigated with the use of compression-moulded samples. It was found that in a certain range of VA content (between 40 and 70%), both impact properties (from 3 to 50–60 kJ m^{-2}) and strain at break (from 4 to 300–350%) highly increased. When the VA content of EVA was low (< 40%) or high (> 70%), the PLA/EVA blend became brittle. The usability of high-VA-content EVA in increasing the ductility of PLA was also demonstrated not only on compression-moulded specimens [27], but also on films [28]. Singla et al. [29] also proved that a strong phase interaction between PLA and EVA exists when 50% VA content was used. At the same time, Cong et al. [30], Aghjeh et al. [31] and Yoon et al. [32], mixed 18%, 18% and 70% VA content EVA with PLA, respectively. However, they achieved only moderate improvement in ductility (either strain or impact strength) even at 20–30 mass% EVA content, due to the lack of compatibility between the phases. Zhang and Lu [33] as well as Ma et al. [34] used 2,5-dimethyl-2,5-di(tert-butylperoxy)hexane as compatibilizer and applied dynamic vulcanization; Moura et al. [35] used transesterification to enhance the compatibility between PLA and EVA, although PLA shows good miscibility with EVA when EVA has a VA content between 40 and 70% [27]. Zhang and Lu [33] investigated a PLA/EVA (70/30 mass%) blend with 28% VA content EVA and pointed out that adding 0.3 mass% compatibilizer greatly increased the impact strength of the blend, from 16.3 to 88.7 kJ m^{-2}. However, even when 0.3 mass% compatibilizer content was fixed and the EVA content was varied, at least 30 mass% EVA was needed to significantly increase ductility, but even at 20 mass% EVA content, it was still only 12.9 kJ m^{-2}.

Finally, Odent et al. [39] investigated the effect of the co-addition of the rubber-like poly(ε-caprolacton-co-lactide) (P(CL-co-LA)) tough copolymer as an impact modifier and N,N′-ethylene bis (12-hydroxystearamide) (EBS) as a nucleating agent. Although the authors did not focus on PLA/EVA blends, they made an important observation, which could also be extended to PLA/EVA blends. Namely, when 10% of a tough copolymer was added to PLA, its notched Izod impact strength of 2.7 kJ m^{-2} increased to 11.4 kJ m^{-2}, but unexpectedly, when 4 mass% of EBS nucleating agent was also added and thus a crystalline structure developed in PLA, the impact strength further increased even up to 30.5 kJ m^{-2}. This could be explained by a possible strong cross-effect between the impact modifier and the crystalline structure of PLA. Finally, this research also highlighted the importance to investigate the synergistic effect of the crystallinity and crystal structure of PLA, and the presence of EVA in PLA/EVA blends.

Finally, to the best of our knowledge, there are no papers investigating the synergistic effect of the various crystal structures of PLA (various ratios of α′ and α crystal forms) and the presence of EVA in injection-moulded and annealed PLA/EVA blends. In our experience, annealing and thus the developed crystal structure can increase the impact strength of PLA. Literature data also indicate that EVA can highly improve toughness and the crystal structure of PLA, and the presence of EVA may have a synergistic effect on impact properties. We prepared various EVA content PLA blends by extrusion and injection moulding and annealed them at different temperatures to develop various crystal structures. Finally, we characterized the annealed PLA/EVA blends by means of calorimetric, thermomechanical and mechanical tests and microscopy.

Experimental

Materials

Injection-moulding-grade PLLA type 3100HP from NatureWorks was used for the experiments with a D-lactide content of around 0.5%. 3100HP PLA has a density of 1.24 g cm^{-3}, a T_g range of 55–60 °C, a melting temperature range of 165–180 °C and a melt flow index of 24 g 10 min^{-1} (at 210 °C, with 2.16 kg load). Based on the literature data of PLA/EVA compatibility, EVA type Levapren 600 from Lanxess was selected and used for the tests with a density of 1.04 g cm^{-3}, a Mooney viscosity of 27 and a VA content of 60%.

Material preparation and processing

We dried PLA at 85 °C for 6 h prior to processing to remove residual moisture and thus to prevent hydrolysis during processing. PLA/EVA blends with an EVA content of 2, 5, 10, 15 and 20 mass% were prepared by twin-screw extrusion. The extruder used was a LabTech Scientific twin-screw extruder (screw diameter = 26 mm, L/D = 40), while a temperature profile of 175–180–185–190 °C (from the hopper to the die) and a screw rotational speed of 10 rpm were applied. The extrudate was pelletized and the pellets of the PLA/EVA blends were injection-moulded with an Arburg Allrounder 370S 700–290 injection-moulding machine equipped with a 30-mm-diameter, L/D = 25 screw. We used an injection rate of 50 cm^3 s^{-1}, a holding pressure of 600 bars, a holding time of 20 s, a residual cooling time of 40 s and melt and mould temperatures of 190 °C and 25 °C, respectively. ISO standard dumb-bell specimens with a cross section of 4 × 10 mm were injection-moulded. Finally, the dumb-bell-shaped specimens were annealed at 80 °C, 100 °C, 120 °C and 140 °C for 1 h in a heat chamber type TYFSF WGL 45B to develop various ratios of α′ and α crystal forms with the possible maximum crystallinity. Some specimens were also left unannealed as reference specimens.

Methods

Differential scanning calorimetry measurements were performed with a TA Instruments Q2000 type calorimeter on 3–6 mg samples taken from the middle of the cross section of the injection-moulded specimens. We investigated the samples in non-isothermal mode (heat/cool/heat) from 0 to 200 °C using a heating/cooling rate of 5 °C min^{-1} to determine the glass transition temperature (T_g), the cold crystallization temperature (T_{cc}), the enthalpy of cold crystallization (ΔH_{cc}), the melting temperature (T_m) and the enthalpy of fusion (ΔH_m) from the heating scan, and the crystallization temperature (T_c) as well as the enthalpy of crystallization (ΔH_c) from the cooling scan. We calculated crystallinity from the first heating scan of the injection-moulded specimens using Eq. (1):

$$X = \frac{\Delta H_m - \Delta H_{cc}}{\Delta H_f \cdot (1 - \alpha)} \cdot 100 \ [\%], \tag{1}$$

where X [%] is the calculated crystallinity, ΔH_m [J g^{-1}] and ΔH_{cc} [J g^{-1}] are the enthalpy of fusion and the enthalpy of cold crystallization, respectively, while ΔH_f [J g^{-1}] is the enthalpy of fusion for 100% crystalline PLA (93.0 J g^{-1}) [40] and α [−] is the mass fraction of EVA.

The mechanical properties were analysed by tensile and Charpy tests. The tensile tests were performed with a Zwick Z020 universal testing machine equipped with a

Zwick BZ 020/TN2S force-measuring cell with a force limit of 20kN and a crosshead speed of 5 mm min^{-1}. The Charpy impact tests were performed on 2-mm-deep notched samples with a Ceast Resil Impactor impact testing machine equipped with a 2-J impact energy hammer and a DAS8000 data collector unit. All of the tests were performed at room temperature at a relative humidity of $50 \pm 10\%$. To grade the ductility of the specimens, we calculated the ductility index (DI) using the following equation:

$$DI = \frac{E_{F_{max}}}{E_{total}} [-], \tag{2}$$

where DI is the ductility index $[-]$, $E_{F_{max}}$ [J] and E_{total} [J] are the energy at maximum force and the total work of fracture, respectively. Subsequently, DI is a dimensionless number between 0 and 1, where 1 represents brittle fracture, while the lower the number, the higher the ductility of the investigated sample.

We examined the specimens with a Jeol JSM 6380LA type scanning electron microscope. The fracture surfaces of the impact specimens were used for the observations. An Au/Pd alloy was sputtered onto the surface prior to observation to avoid electrostatic charging.

The injection-moulded specimens were analysed with a TA Instruments type Q800 Dynamic Mechanical Analyser. We used a dual-cantilever layout to measure the storage modulus above T_g. The heating rate was 2 °C min^{-1} from 0 to 180 °C, the span length was 35 mm, the amplitude was 20 μm, and the frequency was 1 Hz.

Heat Deflection Temperature measurements were performed on a Ceast HV3 type HDT measuring equipment according to the ISO 75 standard. HDT B type measurements were carried out in flatwise mode with a loading stress of 0.45 MPa, heating rate of 2 °C min^{-1} (120 °C h^{-1}) and with a span length of 64 mm.

Results and discussion

As the first step, we performed a DSC investigation of the PLA/EVA blends upon cooling to determine the effect of EVA on the crystallization of PLA (Fig. 1).

Pure PLLA only had a very minor crystallization peak at 97.7 °C representing that even an isotactic PLA only has a slow crystallization rate even at a low cooling rate of 5 °C min^{-1}, and accordingly, its crystallization upon cooling was not complete. At the same time, PLLA has the fastest crystallization rate among higher D-lactide content PLA grades, and thus even a low amount of EVA was able to significantly nucleate it and a definite exothermic peak appeared at 121 °C. Due to the presence of EVA, PLLA fully crystallized during the 5 °C min^{-1} cooling, while
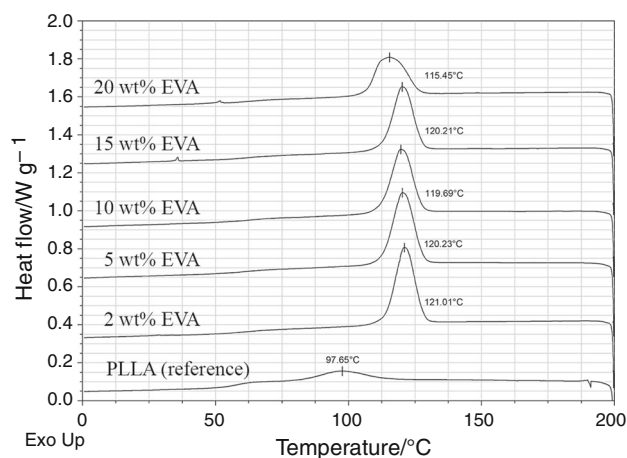

Fig. 1 Cooling DSC scans of unannealed PLA/EVA blends with various EVA contents

pure PLLA could not. These crystallization peaks of the PLA/EVA blends were practically the same for all of the investigated samples, except for the 20 mass% EVA, where a lower nucleation efficiency was found. This predicts that at 20 mass% EVA content, the dispersion of the EVA phase might not be uniform and larger EVA droplets might be found in the PLA matrix decreasing nucleation efficiency. The nucleation efficiency of EVA on PLA was also evident in the first heating scans of the unannealed PLA/EVA samples, since pure PLLA had a cold crystallization peak temperature of 92.9 °C, while EVA shifted this peak temperature to temperatures between 83.7 and 81.6 °C, depending on the EVA content used (Fig. 2).

Due to this nucleation ability of EVA, the crystallinity of the PLA phase increased from 19.6 (pure PLLA) to 29.4%, 40.5%, 35.7%, 38.3% and 36.2% in 2 mass%, 5 mass%, 10 mass%, 15 mass% and 20 mass% EVA content PLA samples, respectively. These values represent
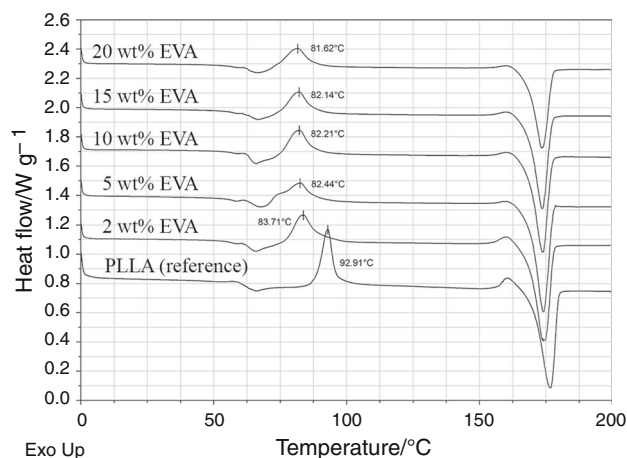

Fig. 2 First heating scan of unannealed PLA/EVA blends with various EVA contents

the crystallinity of the injection-moulded and not annealed specimens as calculated from the first heating scans of the unannealed samples. Although EVA had a significant influence on crystallinity, it had practically no effect on the T_g (63.5 °C ± 0.8 °C) and on the T_m (174.3 °C ± 1.2 °C) of PLA. This suggests that EVA only appears as a dispersed phase in the PLA matrix and the blend is immiscible, but most probably compatible, due to the 60% VA content EVA used. To determine crystallinity and the crystal structure developed during annealing, we also investigated the first heating scan of the annealed PLA/EVA samples (Fig. 3).

15 mass% EVA content was selected as a representative value, since all the other blends behaved in a very similar way. For the pure injection-moulded but unannealed sample, T_g was visible at around 63 °C as well as the cold crystallization exotherm at 92.9 °C, indicating incomplete crystallization during injection moulding. On the contrary, all the annealed samples fully crystallized during the annealing process, which is represented by the absence of cold crystallization exotherm. The crystal melting endotherm was at 176.7 °C, which is that high due to the isotactic structure of PLLA, since with the decrease in D-lactide content, melt temperature increases. Also a small exothermic peak was visible just prior to melting, representing the solid-phase recrystallization of the less ordered α' crystal form into the more ordered α form [26]. This suggests that the crystal structure of the PLLA developed during annealing consists mainly of the less ordered α' crystal form, since it is difficult to develop the more ordered α crystal form in low D-lactide PLA grades (like PLLA) due to its lower T_{cc} compared to higher D-lactide PLA grades [41]. Moreover, although by applying annealing temperatures above 100 °C, the more ordered α could also develop [42], but due to the nucleating effect of

EVA on PLA, the cold crystallization temperatures shifted to even lower temperatures as it was discussed previously (Fig. 2), which promoted the development of the α' crystal form during annealing. At the same time, as annealing temperature was increased, the α'-to-α recrystallization peak shifted to higher temperatures (from 158.7 to 163.3 °C), indicating that the α' crystal form became more and more stable, but still not stable enough to show dual melting peaks of both α' and α crystal forms [43]. Finally, the crystallinity of the annealed samples was practically the same for a certain annealing temperature independently of EVA content. The 15 mass% EVA-filled PLA samples annealed at 80 °C, 100 °C, 120 °C and 140 °C had an average crystallinity of 52.9% ± 0.6%, 52.3% ± 1.9%, 49.9% ± 1.0% and 48.9% ± 0.7%, respectively.

As a next step, we investigated the mechanical (tensile and Charpy impact) properties of the PLA/EVA blends (Figs. 4–7).

As EVA is a low-modulus, low-strength, but high-strain and tough polymer, it decreased both the modulus and strength of the PLA. Adding 20 mass% EVA to PLA
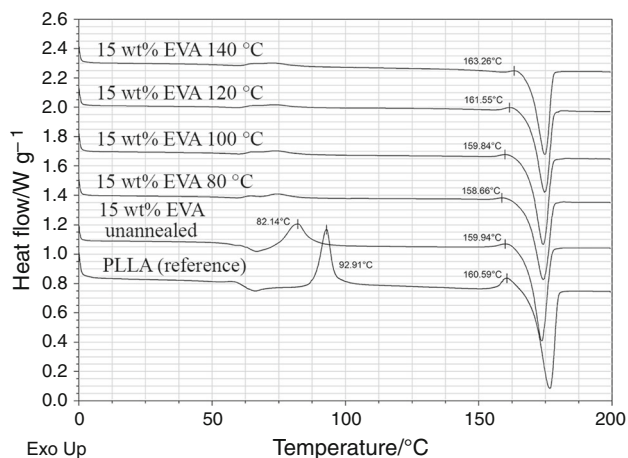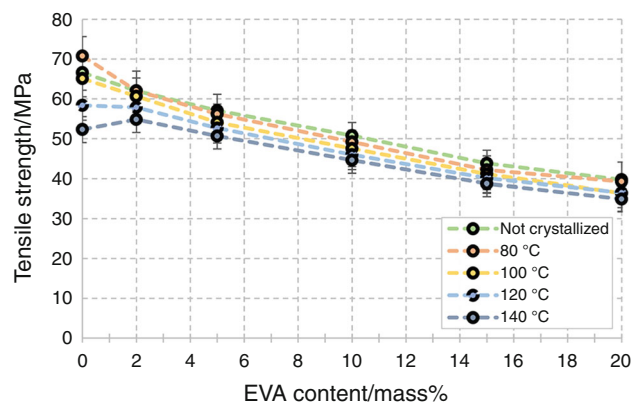

Fig. 4 Tensile strength of the unannealed and annealed PLA/EVA blends

Fig. 5 Tensile modulus of the unannealed and annealed PLA/EVA blends

Fig. 3 First heating scan of 15 mass% EVA content PLA/EVA blends annealed at various temperatures

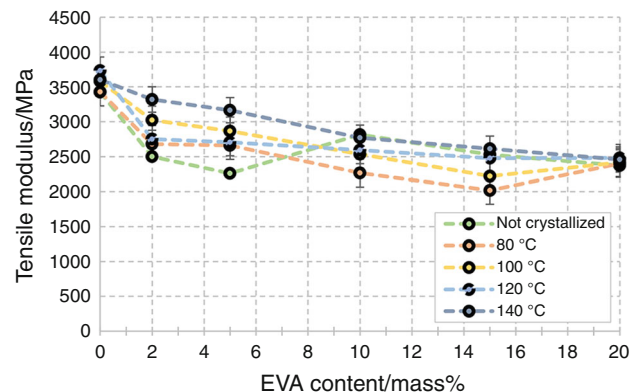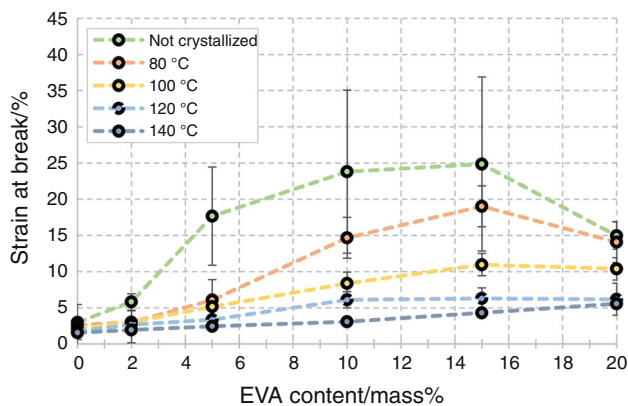**Fig. 6** Strain at break of the unannealed and annealed PLA/EVA blends
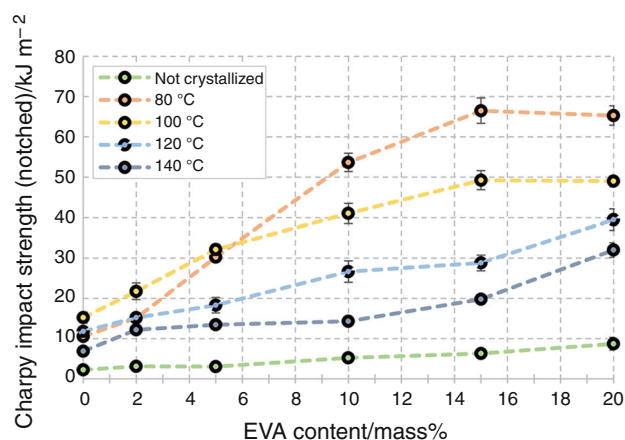
Fig. 7 Notched Charpy impact strength of the unannealed and annealed PLA/EVA blends

Fig. 8 Fracturing process of unannealed PLA, annealed PLA (at 80 °C), unannealed PLA/15 mass%EVA blend and annealed PLA/ 15 mass%EVA blend (at 80 °C). The horizontal scale was only extended to 3.5 ms to show the differences between the curves of the various blends, even though the full fracture of the toughest blend only occurred after 7 ms

decreased its strength and modulus of 66.5 and 3426 MPa–39.7 and 2373 MPa, respectively. Annealing, however, had a different effect on these two mechanical properties—when annealing temperature was increased, strength decreased, while modulus increased. Decreasing strength can be explained with the appearance of more and more microcracks as annealing temperature increases, while the increasing modulus can be explained with the crystal structure that developed and the more and more stable, but still mainly α' crystal form. Regarding the strain at break (Fig. 6) of unannealed PLA/EVA blends, EVA increased the strain of PLA from $3.0 \pm 0.5\%$ to $23.8 \pm 11.3\%$ when 10 mass% EVA was added to PLA, while above this EVA content, the strain of the blends first levelled off then decreased.

This behaviour can be explained by the dispersion of the EVA phase in the PLA matrix. With increasing EVA content, the average size of the EVA droplets most probably increased in the PLA matrix, and their dispersion became less and less uniform. Annealing the PLA/EVA
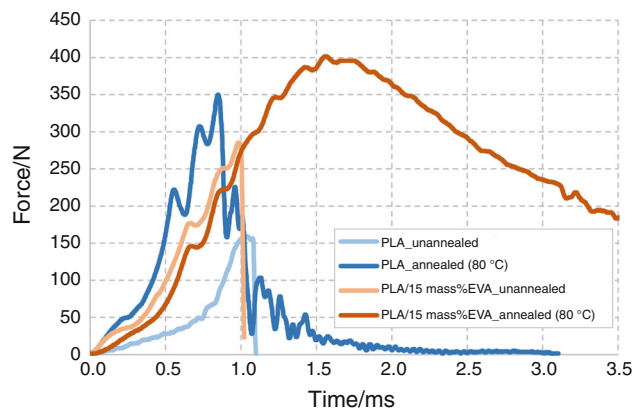
blends decreased the strain values, due to the crystal structure that developed, which could withstand lower strain. If EVA content is simply increased, similar trends can be observed as for the unannealed blends. Unfortunately, at an annealing temperature of 140 °C, even the addition of 20 mass% EVA to PLA only increased strain at break to $5.6\% \pm 0.7\%$.

Concerning impact properties, we found a synergistic effect between the crystal structure of PLA and the presence of EVA (Fig. 7).

When PLA was unannealed, the addition of even 20 mass% EVA only increased impact strength from 2.3 ± 0.6 kJ m^{-2} to 8.7 ± 1.6 kJ m^{-2}. Additionally, when pure PLA was annealed at 100 °C, its impact strength also increased, this time from 2.3 ± 0.6 kJ m^{-2} (unannealed) to 15.2 ± 1.4 kJ m^{-2} due to the crystal structure that developed. When PLA was filled with EVA and annealed at the same time, impact strength increased to over 65 kJ m^{-2}, due to a synergistic toughening mechanism. The highest impact strength of 66.5 kJ m^{-2} ± 3.1 kJ m^{-2} was achieved with 15 mass% of EVA and an annealing temperature of 80 °C. This value is three times higher than the impact strength of ABS (~ 20 kJ m^{-2}), and thus it is very promising in technical applications. When annealing temperature was further increased, impact strength decreased, most probably due to the crack development during higher temperature annealing, as well as due to the appearance of the more and more stable α' crystal form with increasing annealing temperatures. The same trend was found for pure, annealed PLA, where the highest impact strength of 15.2 kJ m^{-2} ± 1.4 kJ m^{-2} was measured after annealing at 100 °C. Above this annealing temperature, impact strength decreased, and after annealing at 140 °C, it was only
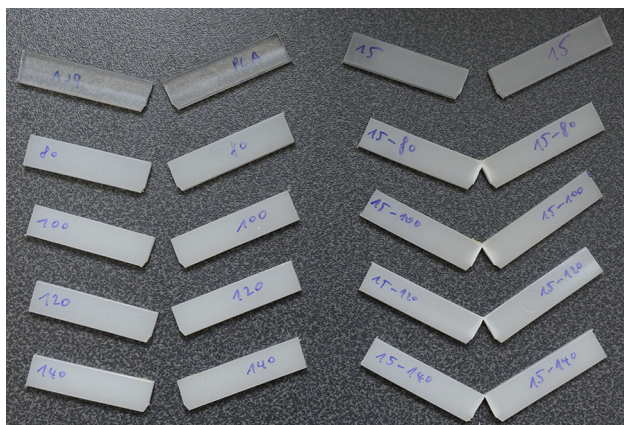
Fig. 9 Charpy-tested fractured specimens. The specimens in the left column from top to bottom are unannealed pure PLA and PLA annealed at 80 °C, 100 °C, 120 °C and 140 °C. The specimens in the right column from top to bottom are unannealed PLA/15 mass%EVA blend and annealed PLA/15 mass%EVA blend at 80 °C, 100 °C, 120 °C and 140 °C
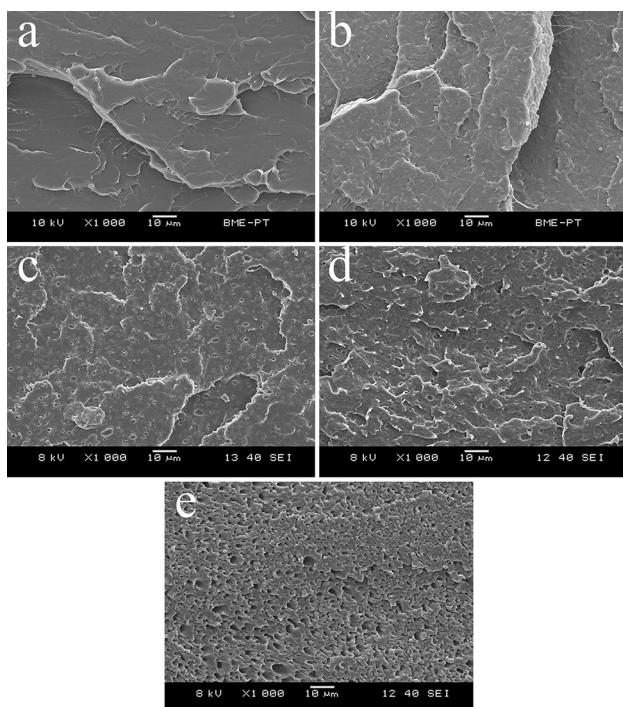

Fig. 10 Charpy fracture surfaces of unannealed PLA (**a**), annealed PLA (**b**), unannealed PLA/15 mass%EVA (**c**), annealed PLA/15 mass%EVA (taken from the middle of the specimen) (**d**) and annealed PLA/15 mass%EVA (taken from near the side of the specimen) (**e**)

6.9 kJ m^{-2} ± 0.4 kJ m^{-2}. The ductility of the annealed and unannealed PLA/EVA blends was also investigated by examining the process of fracture with the use of instrumental impact tests (Fig. 8).

Both unannealed PLA and unannealed PLA/15 mass% EVA specimens had low ductility, meaning that fracture

occurred right after maximum force was reached. Accordingly, their ductility index was 0.94 and 0.91, respectively. On the one hand, annealing pure PLA not only slightly increased maximum force, but also significantly increased ductility (a ductility index of 0.62). Maximum force was reached at 0.85 ms, while full fracture occurred at 2.66 ms. Finally, 15 mass% EVA and annealing at the same time only increased maximum force slightly, but increased the ductility of this blend substantially, even up to a ductility index of 0.38. In this case, during fracture crack most likely propagates along the edges of spherulites causing increased ductility in itself, while it also encounters tough EVA particles, further improving toughness and thus causing the synergistic toughening effect. The fractured specimens are depicted in Fig. 9 demonstrating the nature of the fracture.

The character of the fracture shows the synergistic toughening effect. Due to this synergistic effect, the specimens of pure, unannealed PLA, annealed PLA and unannealed PLA/15 mass%EVA blend suffered full fracture during Charpy impact test, while the specimens of annealed PLA/15 mass%EVA blend did not break. They only suffered partial fracture and stress whitening during the Charpy impact test. Also, the thickness of the unfractured part of the specimens of the annealed PLA/15 mass%EVA blend decreases when annealing temperature is increased. This represents decreasing impact strength as can be seen in the impact strength values (Fig. 7). Next, we observed the fracture surfaces using SEM (Fig. 10).

Unannealed PLA had a typically brittle fracture surface, with sharp edges and flat surfaces (Fig. 10a), while in case of annealed PLA, the fracture surface was rougher, representing higher ductility (Fig. 10b). When 15 mass% EVA was added to PLA and the blend was kept unannealed, the EVA particles were visible as EVA appeared as a finely dispersed phase in the PLA matrix. However, most of them were pulled out during fracture (Fig. 10c). It is also visible that the average particle size was around 2–3 μm. When 15 mass% EVA was added to PLA and the blend was annealed at the same time, its fracture surface indicated far more toughness (Fig. 10d) compared with pure, unannealed PLA. Additionally, in this case, the fracture was represented by two characteristic domains. The first one (image from the middle of the specimen) is represented by round edges and holes of the EVA particles, while in the second one (taken from near the side of the specimen), a very ductile region was found, where PLA suffered high local deformation (Fig. 10e).

We continued by investigating the storage modulus of the PLA/EVA blends (Fig. 11).

The initial storage modulus of unannealed PLA was 2830 MPa at 0 °C, while it kept its high storage modulus up to T_g. Above T_g, modulus decreased drastically as PLA
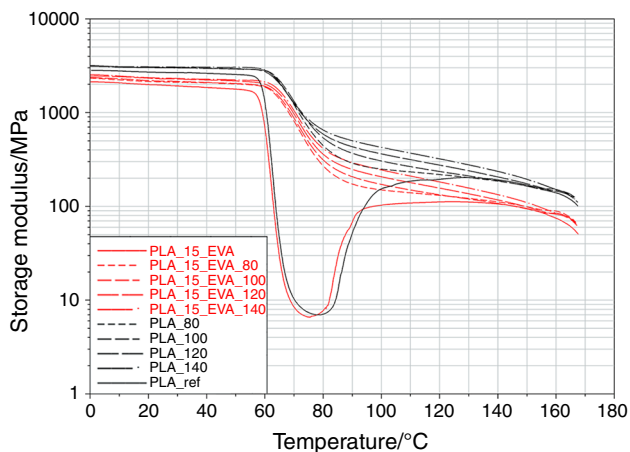
Fig. 11 Storage modulus of the unannealed and annealed pure PLA and 15 mass% EVA content PLA/EVA blends
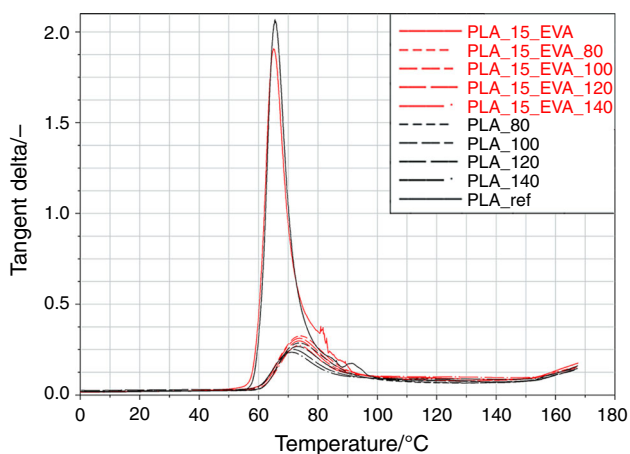

Fig. 12 Tangent delta of the unannealed and annealed pure PLA and 15 mass% EVA content PLA/EVA blends
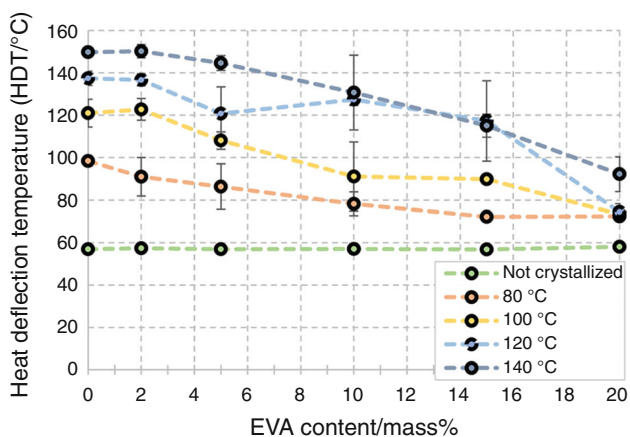

Fig. 13 Heat deflection temperature of unannealed and annealed PLA/EVA blends

entered a rubbery state. The lowest modulus in the rubbery state was 7 MPa at 78 °C. As temperature was further increased, modulus started to increase as cold crystallization took place. After cold crystallization finished, the highest storage modulus reached was 203 MPa at 129 °C. As temperature was further increased, the storage modulus eventually dropped, as temperature was approaching melting temperature. Just prior to melting, there was a small increase, which indicates the α'-to-α crystal form recrystallization. We were able to avoid the drastic drop in storage modulus above T_g by annealing PLA, as crystal structure retarded the micro Brownian motion of polymer chains. Additionally, the higher the annealing temperature was, the higher the storage modulus was due to the more and more ordered crystal structure developing at increasing temperatures. The recrystallization from α' to α also caused an increase in the modulus of the annealed PLA just before melting as well, since the more ordered α crystal form could not fully develop during annealing at any of the applied annealing temperatures. When 15 mass% of EVA was added to PLA and the blend was kept unannealed, the modulus of the blend was naturally lower in the whole investigated temperature range compared to PLA, as EVA is a low-modulus material. The only exception is in the cold crystallization temperature range. Here, due to the nucleating ability of EVA, the increase in storage modulus of the PLA/EVA blend started at lower temperatures, and thus it was higher than the storage modulus of pure PLA between 78 and 94 °C. Additionally, the DSC measurements showed that EVA had a negligible effect on the T_g of PLA, which can be seen on the storage modulus curve as well. As EVA decreased storage modulus, the lowest value of 6.5 MPa was observed at 75 °C, while after cold crystallization finished, the highest value of 112 MPa was found at 125 °C. When the 15 mass% EVA content PLA blends were annealed at various temperatures, very similar storage modulus curves were visible compared to pure, but annealed PLA, but naturally the storage modulus values were lower. The blends that fully entered the rubbery state, namely the unannealed PLA and the PLA/EVA blend, had the highest tan δ of 2.05 and 1.90, respectively, at T_g (Fig. 12).

At the same time, the annealed PLA and PLA/EVA blends had a tan δ from 0.24 to 0.29 and from 0.27 to 0.33, respectively, depending on the annealing temperature. The higher the annealing temperature of the annealed blends was, the lower their tan δ was. At the same time, EVA slightly increased damping even when the blends were annealed.

Finally, we investigated the heat deflection temperature (HDT) of the PLA/EVA blends (Fig. 13).

We found that the HDT of unannealed PLA/EVA blends was independent of the EVA content in the investigated 2–20 mass% EVA content range, which could be explained with the character of storage modulus of the PLA/EVA blends (Fig. 11). Firstly, the HDT of the unannealed PLA is mainly determined by its T_g, where its enters the rubbery state. EVA content had no effect on the T_g of PLA. Secondly, although EVA as a soft phase decreased the modulus of PLA, not even 20 mass% of EVA decreased the inherently high modulus of PLA for the HDT to significantly drop below T_g since PLA remained the major phase in the blends. When pure PLA and the PLA/EVA blends were annealed, the crystal structure that developed ensured significantly higher HDT compared with the unannealed samples. The higher the annealing temperature was, the higher HDT was, due to the more and more stable α' crystal form. Although EVA had no effect on the HDT of unannealed PLA/EVA blends, it decreased the HDT of annealed PLA/EVA blends. The higher the EVA content was, the more it decreased HDT. This is because the soft EVA phase decreases the storage modulus. Since the HDT of the annealed PLA samples was above T_g, the soft EVA phase effectively decreased the overall storage modulus of the PLA/EVA blends to decrease its HDT as well.

As the research results suggested, a crystalline structure in PLA improves both impact properties and HDT, and adding EVA further improves impact properties due to a synergistic toughening effect between the crystal structure of PLA and the presence of EVA. Adding EVA, however, also decreased HDT. Therefore, a balance must be found between the impact properties and the HDT of the PLA/EVA blends to fulfil the requirements of the given application.

Conclusions

We produced ethylene vinyl acetate copolymer (EVA)-filled poly(lactic acid) (PLA) blends using extrusion and injection moulding. We annealed the injection-moulded specimens at 80 °C, 100 °C, 120 °C and 140 °C to develop various crystal structures in PLA. We investigated the cross-effect between the crystal structure of PLA and the presence of EVA on the mechanical, impact, calorimetric and thermomechanical properties, as well as the heat deflection temperature of the blends. Using differential scanning calorimetry (DSC), we proved the nucleating ability of EVA in the low-D-lactide-content PLA (PLLA) used for the experiments. The crystallinity of the PLA phase increased from 19.6% (pure PLLA) to 29.4%, 40.5%, 35.7%, 38.3% and 36.2%, with 2 mass%,

5 mass%, 10 mass%, 15 mass% and 20 mass% EVA content, respectively. The crystal structure of PLLA that developed during annealing consisted of the less ordered α' crystal form, since due to the nucleating effect of EVA on PLA, the cold crystallization temperatures shifted to lower temperatures. This promoted the development of the α' crystal form. As EVA is a low-modulus, low-strength, but high-strain and tough polymer, it decreased the modulus and strength of PLA but increased its strain. We investigated impact properties and found a synergistic effect between the crystal structure of PLA and the presence of EVA. When PLA was unannealed, even 20 mass% EVA only increased its impact strength from 2.3 ± 0.6 kJ m^{-2} to 8.7 ± 1.6 kJ m^{-2}. When pure PLA was annealed at 100 °C, its impact strength increased from 2.3 ± 0.6 kJ m^{-2} (unannealed) to 15.2 ± 1.4 kJ m^{-2}, due to the crystal structure that developed. Annealed PLA/EVA blends, however, had a very high impact strength of over 65 kJ m^{-2}, due to a synergistic toughening mechanism. In this case, during a fracture, crack most likely propagates along the edges of spherulites increasing ductility, while it also encounters tough EVA particles, which further improves toughness. Scanning electron microscopy (SEM) observations confirmed that EVA appeared as a finely dispersed phase in the PLA matrix, with an average particle size around 2–3 μm. Unannealed PLA, annealed PLA and the unannealed PLA/15 mass%EVA blend suffered full fracture during Charpy impact tests, while the specimens of the annealed PLA/15 mass%EVA blend suffered only partial fracture and stress whitening, due to the toughening mechanism. The impact strength of the annealed PLA/EVA blend is more than three times higher than the impact strength of ABS ($\sim$ 20 kJ m^{-2}), and therefore, it holds great promise for technical applications. The heat deflection temperature (HDT) of unannealed PLA/EVA blends, 57 °C, was independent of EVA content in the investigated 2–20 mass% EVA content range. When pure PLA and the PLA/EVA blends were annealed, the crystal structure that developed resulted in significantly higher HDT, between 72 and 140 °C compared to the unannealed samples, depending on EVA content and the annealing temperature. Annealing increased, while EVA content decreased HDT, which could be explained by the crystal structure developing during annealing and the storage modulus decreasing effect of the soft EVA phase, respectively. All results suggested that a crystalline structure in PLA improves both impact properties and HDT. Blending EVA with PLA further improved impact properties due to a synergistic toughening effect between the crystal structure of PLA and the presence of EVA. At the same time, EVA content decreased HDT, consequently, a balance must be found between the impact

properties and the HDT of EVA-filled PLA compounds regarding the requirements of a given application.

Compliance with ethical standards

References

1. Long Y. Biodegradable polymer blends and composites from renewable resources. 1st ed. New Jersey: Wiley; 2009.
2. Srikanth P. Handbook of bioplastics and biocomposites engineering applications. 1st ed. New Jersey: Wiley; 2011.
3. Ren X. Biodegradable plastics: a solution or a challenge? J Clean Prod. 2003;11:27–40. https://doi.org/10.1016/S0959-6526(02)00020-3.
4. Flieger M, Kantorová M, Prell A, Rezanka T, Votruba J. Biodegradable plastics from renewable resources. Folia Microbiol. 2003;48:27–44. https://doi.org/10.1007/BF02931273.
5. Luyt AS. Are biodegradable polymers the solution to the world's environmental problems? Express Polym Lett. 2017;11:764. https://doi.org/10.3144/expresspolymlett.2017.73.
6. Auras R, Lim LT, Selke SEM, Tsuji H. Poly(lactic acid) synthesis, structures, properties, processing and applications. 1st ed. New Jersey: Wiley; 2010.
7. Lim LT, Auras R, Rubino M. Processing technologies for poly(lactic acid). Prog Polym Sci. 2008;33:820–52. https://doi.org/10.1016/j.progpolymsci.2008.05.004.
8. Tábi T, Sajó IE, Szabó F, Luyt AS, Kovács JG. Crystalline structure of annealed polylactic acid and its relation to processing. Express Polym Lett. 2010;4:659–68. https://doi.org/10.3144/expresspolymlett.2010.80.
9. Kulinski Z, Piorkowska E. Crystallisation, structure and properties of plasticized poly(L-lactide). Polymer. 2005;46:10290–300. https://doi.org/10.1016/j.polymer.2005.07.101.
10. Saeidlou S, Huneault MA, Li H, Park CB. Poly(lactic acid) crystallisation. Prog Polym Sci. 2012;37:1657–77. https://doi.org/10.1016/j.progpolymsci.2012.07.005.
11. Pan P, Inoue Y. Polymorphism and isomorphism in biodegradable polyesters. Prog Polym Sci. 2009;34:605–40. https://doi.org/10.1016/j.progpolymsci.2009.01.003.
12. Hoogsteen W, Postema AR, Pennings AJ, ten Brinke G. Crystal structure, conformation, and morphology of solution-spun Poly(L-lactide) fibres. Macromolecules. 1990;23:634–42. https://doi.org/10.1021/ma00204a041.
13. Sasaki S, Asakura T. Helix distortion and crystal structure of the R-form of poly(L-lactide). Macromolecules. 2003;36:8385–90. https://doi.org/10.1021/ma0348674.
14. Zhang J, Duan Y, Sato H, Tsuji H, Noda I, Yan S, Ozaki Y. Crystal modifications and thermal behavior of poly(L-lactic acid) revealed by infrared spectroscopy. Macromolecules. 2005;38:8012–21. https://doi.org/10.1021/ma051232r.
15. Zhang J, Tashiro K, Domb AJ, Tsuji H. Confirmation of disorder α form of poly(L-lactic acid) by the X-ray fiber pattern and polarized IR/Raman spectra measured for uniaxially-oriented samples. Macromol Syst. 2006;242:274–8. https://doi.org/10.1002/masy.200651038.
16. Cho T-Y, Strobl G. Temperature dependent variations in the lamellar structure of poly(L-lactide). Polymer. 2006;47:1036–43. https://doi.org/10.1016/j.polymer.2005.12.027.
17. Puiggali J, Ikada Y, Tsuji H, Cartier L, Okihara T, Lotz B. The frustrated structure of poly(L-lactide). Polymer. 2000;41:8921–30. https://doi.org/10.1016/S0032-3861(00)00235-4.
18. Sawai D, Takahashi K, Sasashige A, Kanamoto T. Preparation of oriented β-form poly(L-lactic acid) by solid-state coextrusion: effect of extrusion variables. Macromolecules. 2003;36:3601–5. https://doi.org/10.1021/ma030050z.
19. Cartier L, Okihara T, Ikada Y, Tsuji T, Puiggali J, Lotz B. Epitaxial crystallization and crystalline polymorphism of polylactides. Polymer. 2000;41:8909–19. https://doi.org/10.1016/S0032-3861(00)00234-2.
20. Tsuji H. Poly(lactide) stereocomplexes: formation, structure, properties, degradation, and applications. Macromol Biosci. 2005;5:569–97. https://doi.org/10.1002/mabi.200500062.
21. Bouapao L, Tsuji H. Stereocomplex crystallization and spherulite growth of low molecular weight Poly(L-lactide) and Poly(D-lactide) from melt. Macromol Chem Phys. 2009;210:993–1002. https://doi.org/10.1002/macp.200900017.
22. Tsuji H, Ikada Y. Stereocomplex formation between enantiomeric poly(lactic acid)s. 9. Stereocomplexation from melt. Macromolecules. 1993;26:6918–26. https://doi.org/10.1021/ma00077a032.
23. Chow WS, Leu YY, Ishak ZAM. Mechanical, thermal and morphological properties of injection molded poly(lactic acid)/calcium carbonate nanocomposites. Period Polytech Mech. 2016;60:15–20. https://doi.org/10.3311/PPme.8319.
24. Rocca-Smith JR, Lagorce-Tachon A, Iaconelli C, Bellat JP, Marcuzzo E, Sensidoni A, Piasente F, Debeaufort F, Karbowiak T. How high pressure CO₂ impacts PLA film properties. Express Polym Lett. 2017;11:320–33. https://doi.org/10.3144/expresspolymlett.2017.31.
25. Chow WS, Teoh EL, Karger-Kocsis J. Flame retarded poly(lactic acid): a review. Express Polym Lett. 2018;12:396–417. https://doi.org/10.3144/expresspolymlett.2018.34.
26. Tábi T, Hajba S, Kovács JG. Effect of crystalline forms (α′ and α) of poly(lactic acid) on its mechanical, thermo-mechanical, heat deflection temperature and creep properties. Eur Polym J. 2016;82:232–43. https://doi.org/10.1016/j.eurpolymj.2016.07.024.
27. Ma P, Hristova-Bogaerds DG, Goossens JGP, Spoelstra AB, Zhang Y, Lemstra PJ. Toughening of poly(lactic acid) by ethylene-co-vinyl acetate copolymer with different vinyl acetate contents. Eur Polym J. 2012;48:146–54. https://doi.org/10.1016/j.eurpolymj.2011.10.015.
28. Xu P, Ma P, Hoch M, Arnoldi E, Cai X, Dong W, Chen M. Transparent blown films from poly(lactide) and poly(ethylene-co-vinyl acetate) compounds: structure and property. Polym Degrad Stab. 2016;129:328–37. https://doi.org/10.1016/j.polymdegradstab.2016.05.010.

29. Singla RK, Zafar MT, Maiti SN, Ghosh AK. Physical blends of PLA with high vinyl acetate containing EVA and their rheological, thermo-mechanical and morphological responses. Polym Test. 2017;63:398–406. https://doi.org/10.1016/j.polymertesting.2017.08.042.

30. Cong DV, Hoang T, Giang NV, Ha NT, Lam TD, Sumita M. A novel enzymatic biodegradable route for PLA/EVA blends under agricultural soil of Vietnam. Mater Sci Eng C. 2012;32:558–63. https://doi.org/10.1016/j.msec.2011.12.012.

31. Aghjeh MR, Nazari M, Khonakdar HA, Jafari SH, Wagenknecht U, Heinrich G. In depth analysis of micro-mechanism of mechanical property alternations in PLA/EVA/clay nanocomposites: a combined theoretical and experimental approach. Mater Des. 2015;88:1277–89. https://doi.org/10.1016/j.matdes.2015.09.081.

32. Yoon J-S, Oh S-H, Kim M-N, Chin I-J, Kim Y-H. Thermal and mechanical properties of poly(L-lactic acid)–poly (ethylenecovinyl acetate) blends. Polymer. 1999;40:2303–12. https://doi.org/10.1016/S0032-3861(98)00463-7.

33. Zhang N, Lu X. Morphology and properties of super-toughened bio-based poly(lactic acid)/poly(ethylene-co-vinyl acetate) blends by peroxide-induced dynamic vulcanization and interfacial compatibilization. Polym Test. 2016;56:354–63. https://doi.org/10.1016/j.polymertesting.2016.11.003.

34. Ma P, Xu P, Zhai Y, Dong W, Zhang Y, Chen M. Biobased Poly(lactide)/ethylene-co-vinyl acetate thermoplastic vulcanizates: morphology evolution, superior properties, and partial degradability. ACS Sustain Chem Eng. 2015;3:2211–9. https://doi.org/10.1021/acssuschemeng.5b00462.

35. Moura I, Nogueira R, Bounor-Legare V, Machado AV. Synthesis of EVA-g-PLA copolymers using transesterification reactions. Mater Chem Phys. 2012;134:103–10. https://doi.org/10.1016/j.matchemphys.2012.02.036.

36. Salyer IO, Kenyon AS. Structure and property relationships in ethylene–vinyl acetate copolymers. J Polym Sci Pol Chem. 1971;9:3083–103. https://doi.org/10.1002/pol.1971.150091101.

37. Gajria AM, Davé V, Gross RA, McCarthy SP. Miscibility and biodegradability of blends of poly(lactic acid) and poly(vinyl acetate). Polymer. 1996;37:437–44. https://doi.org/10.1016/0032-3861(96)82913-2.

38. Anderson KS, Hillmyer MA. The influence of block copolymer microstructure on the toughness of compatibilized polylactide/polyethylene blends. Polymer. 2004;45:8809–23. https://doi.org/10.1016/j.polymer.2004.10.047.

39. Odent J, Raquez J-M, Leclére P, Lauro F, Dubois P. Crystallization-induced toughness of rubber-modified polylactide: combined effects of biodegradable impact modifier and effective nucleating agent. Polym Adv Technol. 2015;26:814–22. https://doi.org/10.1002/pat.3513.

40. Battegazzore D, Bocchini S, Frache A. Crystallisation kinetics of poly(lactic acid)-talc composites. Express Polym Lett. 2011;5:849–58. https://doi.org/10.3144/expresspolymlett.2011.84.

41. Tábi T, Wacha AF, Hajba S. Effect of D-Lactide content of annealed poly(lactic acid) on its thermal, mechanical, heat deflection temperature, and creep properties. J Appl Polym Sci. 2018;10:47103. https://doi.org/10.1002/app.47103.

42. Zhang J, Tashiro K, Tsuji H, Domb AJ. Disorder-to-order phase transition and multiple melting behavior of Poly(L-lactide) investigated by simultaneous measurements of WAXD and DSC. Macromolecules. 2008;41:1352–7. https://doi.org/10.1021/ma0706071.

43. Pan P, Kai W, Zhu B, Dong T, Inoue Y. Polymorphous crystallization and multiple melting behavior of Poly(L-lactide): molecular weight dependence. Macromolecules. 2007;40:6898–905. https://doi.org/10.1021/ma071258d.